

Solvent Controlled Self-Assembly at the Liquid-Solid Interface Revealed by STM

Wael Mamdouh,[†] Hiroshi Uji-i,[†] Janine S. Ladislav,[‡] Andres E. Dulcey,[‡]
Virgil Percec,[‡] Frans C. De Schryver,[†] and Steven De Feyter^{*†}

Contribution from the Department of Chemistry, Division of Molecular and Nano Materials, Laboratory of Photochemistry and Spectroscopy, Katholieke Universiteit Leuven, Celestijnenlaan 200-F, 3001 Leuven, Belgium, and Department of Chemistry, Roy and Diana Vagelos Laboratories, University of Pennsylvania, Philadelphia, Pennsylvania 19104-6323

Received September 8, 2005; E-mail: Steven.DeFeyter@chem.kuleuven.be

Abstract: The effect of solvent on the two-dimensional (2D) supramolecular ordering of monodendron 1 at the liquid-solid interface has been systematically investigated by means of scanning tunneling microscopy (STM). Solvents range from those with hydrophilic solvating properties, such as alkylated alcohols and acids, to hydrophobic solvents such as alkylated aromatics and alkanes. Dramatic differences in the 2D ordering are observed depending on the nature of the solvent. Of particular interest is the fact that in hydrophobic solvating solvents, such as aliphatic and aromatic hydrocarbons, solvent molecules are coadsorbed in the 2D molecular network while this is not the case for alkylated alcohols or acids. Furthermore, in the case of the coadsorbing solvents, a striking influence of the alkyl chain length has been observed on the 2D pattern formed. The solvent and alkyl chain length dependences are discussed in terms of molecule–molecule interactions (homo and hetero) and molecule–substrate interactions.

1. Introduction

Controlling the 2D pattern formation of molecules or mixtures of molecules at surfaces¹ by exploiting noncovalent interactions such as hydrogen bonding² and metal-coordination³ chemistry is an active area of research. The liquid-solid interface is an ideal environment to induce the 2D self-assembly by physisorption under thermodynamic control. STM has proven to be a powerful technique to image and study these types of physisorbed layers at the liquid-solid interface, focusing on the role of noncovalent interactions, dynamics, and reactivity. However, few reports deal with the influence of solvent on the pattern formation at the liquid–solid interface, though this is potentially an important approach for controlling the 2D supramolecular structures.⁴

The organic solvents used at the liquid-solid interface often comply with the following criteria: (1) they have a low vapor pressure allowing the performance of the STM measurements in only a drop of liquid without the need of a closed cell, (2) they are electrochemically inert under the experimental conditions, (3) they solubilize the compound of interest, and (4) they have a low affinity for adsorption on the substrate used.

Flynn et al. reported that solvents could play an appreciable role in the adsorption and mobility of triacontane/triacontanol molecules adsorbed on the graphite surface.⁵ In the case of physisorbed monolayers of trimesic acid (TMA) formed at the interface of the surface of highly oriented pyrolytic graphite (HOPG) and solutions of TMA in a homologous series of alkanolic acid solvents (butyric to nonanoic acid),⁶ different polymorphs were observed depending on the solvent used.^{2g}

From mixed solutions, mixed monolayers can be formed, leading to two different situations: (1) the different molecules organize in separate domains,^{5,7} or (2) they form mixed domains, which sometimes leads to the formation of mixed 2D crystals.^{2a,i,l,8} Though it is not usually a main goal, solvent molecules can coadsorb inside the 2D molecular network, even if they do not form stable physisorbed monolayers themselves under the same experimental conditions.^{4,9}

[†] Katholieke Universiteit Leuven.

[‡] University of Pennsylvania.

- (1) De Feyter, S.; De Schryver, F. C. *Chem. Soc. Rev.* **2003**, *32* (3), 139–150.
(2) (a) De Feyter, S.; Gesquière, A.; Abdel-Mottaleb, M. M.; Grim, P. C. M.; De Schryver, F. C.; Meiners, C.; Sieffert, M.; Valiyaveetil, S.; Müllen, K. *Acc. Chem. Res.* **2000**, *33* (8), 520–531. (b) Lei, S. B.; Wang, C.; Yin, S. X.; Wang, H. N.; Xi, F.; Liu, H. W.; Xu, B.; Wan, L. J.; Bai, C.-L. *J. Phys. Chem. B* **2001**, *105*, 10838–10841. (c) Giancarlo, L. C.; Flynn, G. W. *Acc. Chem. Res.* **2000**, *33*, 491–501. (d) Xie, Z. X.; Charlier, J.; Cousty, J. *Surf. Sci.* **2000**, *448*, 201–211. (e) Barth, J. V.; Weckesser, J.; Cai, C. Z.; Günter, P.; Burgi, L.; Jeandupeux, O.; Kern, K. *Angew. Chem.* **2000**, *112*, 1285–1288. (f) Barth, J. V.; Weckesser, J.; Cai, C.; Günter, P.; Bürgi, L.; Jeandupeux, O.; Kern, K. *Angew. Chem., Int. Ed.* **2000**, *39*, 1230–1234. (g) Griessl, S.; Lackinger, M.; Edelwirth, M.; Hietschold, M.; Heckl, W. M. *Single Molecules* **2002**, *3*, 25–31. (h) Kim, Y. G.; Yau, S. L.; Itaya, K. *Langmuir* **1999**, *15*, 7810–7815. (i) Theobald, J. A.; Oxtoby, N. S.; Philips, M. A.; Champness, N. R.; Beton, P. H. *Nature* **2003**, *424*, 1029–1031. (j) De Feyter, S.; Gesquière, A.; Klapper, M.; Müllen, K.; De Schryver, F. C. *Nano Lett.* **2003**, *3*, 1485. (k) Keeling, D. L.; Oxtoby, N. S.; Wilson, C.; Humphry, M. J.; Champness, N. R.; Beton, P. H. *Nano Lett.* **2003**, *3*, 9–12. (l) Kampschulte, L.; Griessl, S.; Heckl, W. M.; Lackinger, M. *J. Phys. Chem. B* **2005**, *109*, 14074.
(3) Semenov, A.; Spatz, J. P.; Möller, M.; Lehn, J.-M.; Sell, B.; Schubert, D.; Weidl, C. H.; Schubert, U. S. *Angew. Chem., Int. Ed.* **1999**, *38*, 2547.

- (4) (a) Vanoppen, P.; Grim, P. C. M.; Rücker, M.; De Feyter, S.; Moessner, G.; Valiyaveetil, S.; Müllen, K.; De Schryver, F. *J. Phys. Chem.* **1996**, *100*, 19636–19641. (b) Li, C.-J.; Zeng, Q.-D.; Wang, C.; Wan, L.-J.; Xu, S.-L.; Wang, C.-R.; Bai, C.-L. *J. Phys. Chem. B* **2003**, *107*, 747–750. (c) Yablon, D. G.; Wintgens, D.; Flynn, G. W. *J. Phys. Chem. B* **2002**, *106*, 5470–5475.
(5) Venkataraman, B.; Breen, J. J.; Flynn, G. W. *J. Phys. Chem.* **1995**, *99*, 6608.
(6) Lackinger, M.; Griessl, S.; Heckl, W. M.; Hietschold, M.; Flynn, G. W. *Langmuir* **2005**, *21*, 4984.

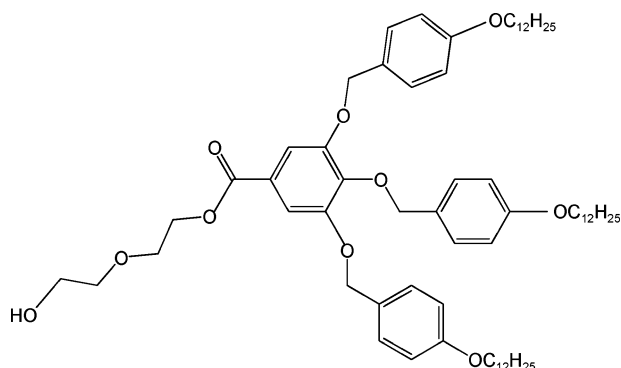


Figure 1. Chemical structure of monodendron **1**.

Monodendrons have been rationally designed and synthesized in such a way that they self-assemble through various molecular recognition mechanisms into rodlike,¹⁰ cylindrical,¹¹ and spherical¹² supramolecular dendrimers. These molecules also form self-assembled physisorbed monolayers at the liquid–solid interface. In this contribution, we report on a systematic study of the role played by solvent molecules on the self-assembly of an alkylated monodendron **1** (Figure 1) at the liquid–solid interface. The selected solvents range from unsubstituted alkanes to substituted alkanes with an OH group (alcohol), COOH group (acid), or phenyl group at the 1-position. In some cases, such as in phenyl alkanes, solvent codeposition was observed while for OH and COOH functionalized alkanes no coadsorption was detected. Surprisingly, upon increasing the chain length of the phenyl alkanes, the number of coadsorbed solvent molecules per monodendron increases, and therefore, the 2D supramolecular patterns are affected accordingly. We discuss the solvent dependence on the formation of the molecular adlayers in terms of the solubilizing properties of the solvents, solvent–solvent interactions, molecular shape and dimension of the solvent, and packing constraints.

2. Experimental Section

The synthesis and structural analysis of monodendron **1** (3,4,5-tris-(4-dodecyloxy-benzyloxy)-benzoic acid 2-(2-hydroxy-ethoxy)-ethyl ester (CAS number: 153733-02-9)) are detailed elsewhere.¹³

STM experiments were performed using a Discoverer Scanning Tunneling Microscope (Topometrix Inc., Santa Barbara, CA) along with

- (7) (a) Stevens, F.; Dyer, D. J.; Walba, D. M. *Langmuir* **1996**, *12*, 436. (b) Hippias, K. W.; Lu, X.; Wang, X. D.; Mazur, U. *J. Phys. Chem.* **1996**, *100*, 11207. (c) Baker, R. T.; Mougous, J. D.; Brackley, A.; Patrick, D. L. *Langmuir* **1999**, *15*, 4884. (d) Padowitz, D. F.; Sada, D. M.; Kemer, E. L.; Dougan, M. L.; Xue, W. A. *J. Phys. Chem. B* **2002**, *106*, 593. (e) De Feyter, S.; Larsson, M.; Schuurmans, N.; Verkuijl, B.; Zorinians, G.; Gesquière, A.; Abdel-Mottaleb, M. M.; van Esch, J.; Feringa, B. L.; van Stam, J.; De Schryver, F. C. *Chem.–Eur. J.* **2003**, *9*, 198.
- (8) (a) Eichhorst-Gerner, K.; Stabel, A.; Moessner, G.; Declercq, D.; Valiyaveetil, S.; Enkelmann, V.; Müllen, K.; Rabe, J. P. *Angew. Chem., Int. Ed. Engl.* **1996**, *35*, 1492. (b) Qian, P.; Nanjo, H.; Yokoyama, T.; Suzuki, T. M.; Akasaka, K.; Orhui, H. *Chem. Commun.* **2000**, 2021. (c) Wintgens, D.; Yablon, D. G.; Flynn, G. W. *J. Phys. Chem. B* **2003**, *107*, 173. (d) Yang, X.; Mu, Z.; Wang, Z.; Zhang, X.; Wang, J.; Wang, Y. *Langmuir* **2005**, *21*, 7225.
- (9) Gyafas, B. J.; Wiggins, B.; Zosel, M.; Hippias, K. W. *Langmuir* **2005**, *21*, 919.
- (10) Percec, V.; Chu, P.; Ungar, G.; Zhou, J. *J. Am. Chem. Soc.* **1995**, *117*, 11441.
- (11) (a) Percec, V.; Johansson, G.; Ungar, G.; Zhou, J. *J. Am. Chem. Soc.* **1996**, *118*, 9855 and references therein. (b) Percec, V.; Ahn, C.-H.; Ungar, G.; Yearley, D. J. P.; Moeller, M.; Sheiko, S. S. *Nature* **1998**, *391*, 161. (c) Percec, V.; Glodde, M.; Bera, T. K.; Miura, Y.; Shiyankovskaya, I.; Singer, K. D.; Balagurusamy, V. S. K.; Heiney, P. A.; Schnell, I.; Rapp, A.; Spiess, H.-W.; Hudson, S. D.; Duan, H. *Nature* **2002**, *419*, 384. (d) Percec, V.; Dulcey, A. E.; Balagurusamy, V. S. K.; Miura, Y.; Smidrkal, J.; Peterca, M.; Nummelin, S.; Edlund, U.; Hudson, S. D.; Heiney, P. A.; Duan, H.; Magonov, S. N.; Vinogradov, S. A. *Nature* **2004**, *430*, 764.

Scheme 1. Different Classes of Solvents and Their Chemical Structures

Solvent Class	Chemical structures	
Class A	HO-(CH ₂) _n -H	n = 7 (1-heptanol) n = 8 (1-octanol)
	HOOC-(CH ₂) _n -H	n = 7 (1-octanoic acid)
Class B	-(CH ₂) _n -H	n = 7 (1-phenylheptane) n = 8 (1-phenyloctane) n = 10 (1-phenyldecane) n = 12 (1-phenyldodecane) n = 14 (1-phenyltetradecane)
	H-(CH ₂) _n -H	n = 12 (dodecane) n = 14 (tetradecane)

an external pulse/function generator (Model HP 8111 A), with a negative sample bias. Tips were electrochemically etched from Pt/Ir wire (80%/20%, diameter 0.2 mm) in 2 N KOH/6 N NaCN solution in water. Prior to imaging, monodendron **1** was dissolved in two classes of solvents. Class A contains alkylated solvents with hydrophilic solvating properties, i.e., with a hydroxyl group (OH) or carboxylic acid group (COOH), such as 1-heptanol, 1-octanol, and 1-octanoic acid (Aldrich 99%). Class B consists of alkylated hydrophobic solvents, including alkanes such as dodecane and tetradecane, and a series of phenyl substituted alkanes, including 1-phenylheptane, 1-phenyloctane, 1-phenyldecane, 1-phenyldodecane, and 1-phenyltetradecane (Aldrich 99%). The solutions of monodendron **1** in the chosen solvents were prepared at a concentration of approximately 1 mg/gr. Then, a drop of the solution was applied onto a freshly cleaved surface of highly oriented pyrolytic graphite (HOPG, grade ZYB, Advanced Ceramics Inc., Cleveland, OH). The STM tip was immersed in solution, and images were recorded at the liquid–solid interface. The STM images were acquired in the variable-current mode (constant height). The measured tunneling currents are converted into a gray scale: black (white) refers to a low (high) measured tunneling current. The experiments were repeated in several sessions using several tips to check for reproducibility and to avoid artifacts. For analysis purposes, recording of a monolayer image was followed by imaging the graphite substrate underneath under the same experimental conditions, except for lowering the bias voltage. The images were corrected for drift via Scanning Probe Image Processor (SPIP) software (Image Metrology ApS), using the recorded graphite images for calibration purposes, allowing a more accurate unit cell determination. The imaging parameters are indicated in the figure captions: tunneling current (*I*), and sample bias (*V*).

The molecular models were made using HyperChem. They are not meant to be a true representation of the molecular conformation and two-dimensional ordering. Except if stated otherwise in the text, they only indicate the location of the phenyl groups and alkoxy chains of the monodendrons (not the specific orientation) and the location of the coadsorbed solvent molecules (see text for more details).

3. Results

In this study, the solvents are grouped as follows (Scheme 1): Class A contains solvents with hydrophilic functional groups such as a hydroxyl group (1-heptanol and 1-octanol) or a

- (12) (a) Balagurusamy, V. S. K.; Ungar, G.; Percec, V.; Johansson, G. *J. Am. Chem. Soc.* **1997**, *119*, 1539. (b) Ungar, G.; Liu, Y.; Zeng, X.; Percec, V.; Cho, W.-D. *Science* **2003**, *299*, 1208. (c) Zeng, X.; Ungar, G.; Liu, Y.; Percec, V.; Dulcey, A. E.; Hobbs, J. K. *Nature* **2004**, *428*, 157.
- (13) (a) Mamdouh, W.; Uji-I, H.; Dulcey, A. E.; Percec, V.; De Feyter, S.; De Schryver, F. C. *Langmuir* **2004**, *20*, 7678. (b) Percec, V.; Heck, J.; Tomazos, D.; Falkenberg, F.; Blackwell, H.; Ungar, G. *J. Chem. Soc., Perkin Trans. 1* **1993**, *1*, 2799.

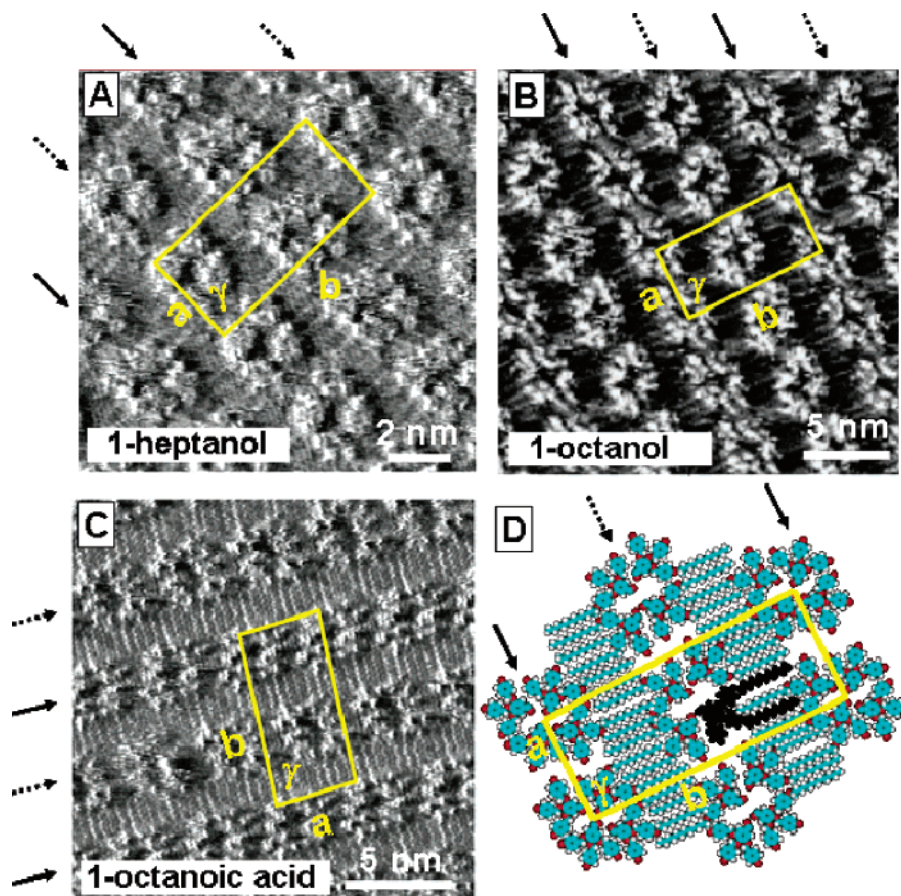


Figure 2. STM images of monolayers of **1** physisorbed at the liquid–HOPG interface from class A solvents. (A) The solvent is 1-heptanol. $I_t = 0.65$ nA; $V_t = -0.466$ V. (B) The solvent is 1-octanol. $I_t = 0.85$ nA; $V_t = -0.606$ V. (C) The solvent is 1-octanoic acid. $I_t = 0.8$ nA; $V_t = -0.444$ V. (D) Tentative molecular model reflecting the ordering in B but representing the molecular organization obtained from all class A solvents. The difference in orientation of the tetramers from row to row is indicated by solid and dotted arrows, respectively. Unit cells are indicated in yellow. One monodendron is indicated in black (the alkyl chains are directed to the solution phase, and the oligoether parts are omitted).

carboxylic acid group (1-octanoic acid). Class B contains *n*-alkanes (dodecane and tetradecane) and other hydrophobic alkanes with different chain lengths. Also included in Class B are phenyl-substituted alkanes.

3.1. Self-Assembly upon Adsorption from Solvents of Class A. Figure 2A–C represent STM images of physisorbed monolayers of monodendron **1** formed upon applying a drop of **1** dissolved in 1-heptanol, 1-octanol, and 1-octanoic acid, respectively, onto a freshly cleaved HOPG surface. **1** shows very similar 2D supramolecular patterns in these solvents. A model reflecting the molecular ordering shown in Figure 2B, which is representative for the molecular organization obtained in all class A solvents, is presented in Figure 2D. Domains which extend over several hundreds of square nanometers (see also Figure S1 in the Supporting Information). Highly regular patterns are observed. In the STM images, aromatic moieties are often observed to show a higher tunneling efficiency¹⁴ allowing a straightforward interpretation of the bright-dark contrast in the images. Therefore, the larger bright structures (spots) correspond to the phenyl rings in monodendron **1**. Not all phenyl groups appear with the same brightness, indicating that they do not have the same orientation with respect to the graphite substrate. Different tilt angles of the phenyl rings are

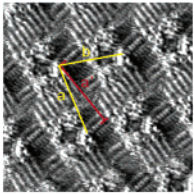
expected to result in differences in contrast. The graylike striped features correspond to the alkyl chains.

Upon physisorption from class A solvents, monodendron **1** forms “cyclic” tetramers with a “dark” center (cavity). The formation of tetramers might involve hydrogen bonding between the carbonyl group of one monodendron and the hydroxyl group of another monodendron. The tetramers appear distorted, and from row to row, the orientation of the tetramers alternates. This is indicated by the sequence of arrows in Figure 2. Rows of tetramers are separated by alkyl chains which run almost perpendicular to these rows. The distance between adjacent rows is calculated to be 3.9 nm, which equals the unit cell parameter *b* divided by 2, and indicates that the alkyl chains adopt an extended zigzag conformation though being interdigitated. They run parallel to one of the main graphite axes underneath ($\langle 01\bar{1}0 \rangle$) revealing the adsorbate–substrate interaction.¹⁵ The distance between two adjacent alkyl chains is approximately 0.46 nm. Images such as that in Figure 2C reveal the presence of eight alkyl chains per tetramer along unit cell vector *b*, indicating that the other four alkyl chains should be oriented along unit cell vector *a*. However, the latter alkyl chains could not be observed. This agrees with the distance between the tetramers along unit cell vector *a* (3.9 nm), which is too small for the

(14) Lazzaroni, R.; Calderone A.; Lambin, G.; Rabe, J. P.; Brédas, J. L. *Synth. Met.* **1991**, *41–43*, 525.

(15) Kaneda, Y.; Stawasz, M.; E.; Sampson, D. L.; Parkinson, B. A. *Langmuir* **2001**, *17*, 6185.

Table 1. Unit Cell Parameters and Other Characteristic Parameters of Adlayers of Monodendron **1** in the Different Solvents Studied^a

Class		Unit cell parameters			Number of monodendrons per unit cell	Unit cell area (nm ²)	Unit cell area (nm ²)/N _m	Number of alkyl chains along <i>b</i>	Number of alkyl chains along <i>a</i>	Number of co-adsorbed solvent molecules per tetramer	
		<i>a</i> (nm)	<i>b</i> (nm)	γ (°)							
Solvent ^b		<i>a</i> (nm)	<i>b</i> (nm)	γ (°)	N _m	A	A _m	<i>a'</i> (nm)	N _b	N _a	S _T
A	1-heptanol	3.8 ± 0.1	7.9 ± 0.1	89 ± 2	8	30 ± 1	3.8 ± 0.1	3.8 ± 0.1	8	4	0
	1-octanol	3.9 ± 0.1	8.0 ± 0.1	87 ± 2	8	31 ± 1	3.9 ± 0.1	3.8 ± 0.1	8	4	0
	1-octanoic acid	3.9 ± 0.1	7.8 ± 0.1	89 ± 1	8	30 ± 1	3.8 ± 0.1	3.8 ± 0.1	8	4	0
B	1-phenylheptane	4.6 ± 0.1	4.7 ± 0.1	61 ± 2	4	19.0 ± 0.4	4.8 ± 0.1	4.6 ± 0.1	10	4	2
	1-phenyloctane	4.7 ± 0.1	4.7 ± 0.1	60 ± 2	4	19.0 ± 0.4	4.8 ± 0.1	4.5 ± 0.1	10	4	2
	1-phenyldecane	4.7 ± 0.4	4.7 ± 0.4	60 ± 10	4	19.1 ± 2.2	4.8 ± 0.5	4.6 ± 0.4	10	4	2
	1-phenyldodecane	4.7 ± 0.1	4.7 ± 0.1	70 ± 2	4	20.8 ± 0.6	5.2 ± 0.2	4.7 ± 0.1	10	5	3
		6	4								
1-phenyltetradecane	4.8 ± 0.1	4.8 ± 0.1	60 ± 2	4	20.0 ± 0.4	5.0 ± 0.1	4.8 ± 0.1	11	5	4	
	4.8 ± 0.1	4.8 ± 0.1	79 ± 2		22.6 ± 0.8	5.7 ± 0.2	4.6 ± 0.1	10	8	6	

^a *a, b, γ* = unit cell parameters. *a'* = distance as indicated in the figure in the top of the table (running perpendicular to the long axis of the alkyl chains). N_m = number of monodendrons per unit cell. A = unit cell area (nm²). A_m = unit cell area divided by number of monodendrons per unit cell area. N_b = value of the number of alkyl chains perpendicular to unit cell vector *a* obtained either by counting if the image contrast allows or by rounding the value of *a'* divided by 0.46 to the nearest number. N_a = value of the number of alkyl chains along unit cell vector *a*. S_T = number of coadsorbed solvent molecules per tetramer. ^b The resolution of the images in dodecane and tetradecane do not allow an accurate determination of the unit cell vectors and the other packing parameters.

alkyl chains to bridge the gap between two adjacent tetramers while adopting an extended conformation. These alkyl chains along unit cell vector *a* are most likely directed toward the solution phase, at least in part. Unit cells are indicated in yellow in Figure 2. They contain eight monodendrons. The unit cell parameters are similar in these solvents: *a* = 3.9 nm, *b* = 7.9 nm, and γ = 88° (see also Table 1).

3.2. Self-Assembly upon Adsorption from Solvents of Class B. In phenyl-substituted alkanes monolayers are formed as well, though the 2D ordering differs significantly from that obtained in class A solvents.

From 1-Phenylheptane to 1-Phenyldecane: Figures 3A–C show some representative STM images of physisorbed monolayers of **1** at the 1-phenylheptane–, 1-phenyloctane–, and 1-phenyldecane–graphite interface, respectively (see also Figure S2 in the Supporting Information for large area images). Figure 3D is a tentative molecular model reflecting the molecular

ordering in Figure 3B, which is representative for the molecular organization in all three solvents mentioned (see also Table 1). Similar to the molecular packing observed for **1** in class A solvents, cyclic tetramers are observed. However, the tetramers appear to be more symmetrical, and no tilt was observed from one row to the other. The alkyl chains are interdigitated, separated by approximately 0.46 nm, and can be divided into two subsets depending on their orientation and contrast. Those two subsets are oriented perpendicular to each other. From every monodendron, two fully extended alkyl chains are oriented almost perpendicularly to the unit cell vector *a*, and those alkyl chains are oriented along one of the main symmetry axes of the graphite lattice underneath, which is similar to the ordering in class A solvents. The third alkyl chain of each monodendron, which was not observed in class A solvents, is now oriented along unit cell vector *a*, is fully extended, and appears sometimes brighter than the other alkyl chains (e.g., Figure 3B). As a result,

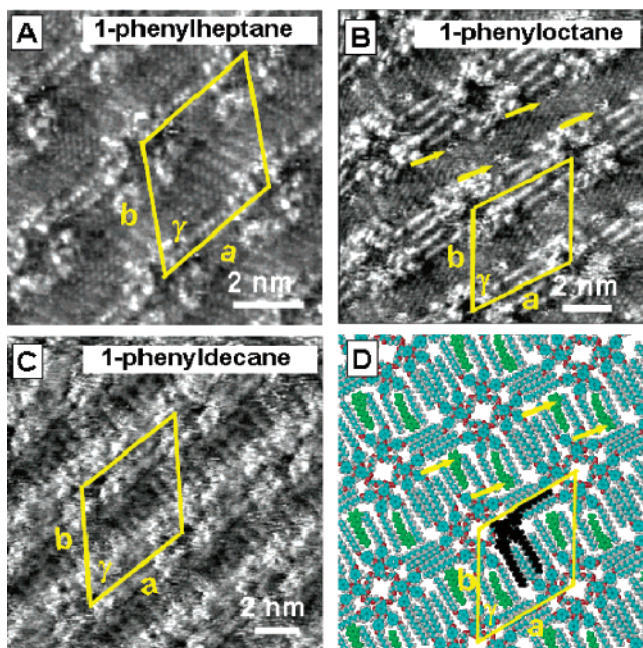


Figure 3. STM images of monolayers of **1** physisorbed at the liquid–HOPG interface from class B solvents. (A) The solvent is 1-phenylheptane. $I_t = 0.5$ nA; $V_t = -0.676$ V. (B) The solvent is 1-phenyloctane. $I_t = 0.5$ nA; $V_t = -0.518$ V. Additional bright features are observed (yellow arrows) indicating coadsorption of 1-phenyloctane molecules. (C) The solvent is 1-phenyldecane. $I_t = 0.8$ nA; $V_t = -0.906$ V. (D) Tentative molecular model reflecting the ordering in B, at the 1-phenyloctane–graphite interface, but representing the molecular organization obtained in the other solvents too. The 1-phenyloctane molecules are colored in green, and the location of the phenyl groups is indicated with yellow arrows. Unit cells are indicated in yellow. One monodendron is indicated in black.

along this direction there are four of the latter type of alkyl chains between two adjacent tetramers. The difference in contrast between the alkyl chains can be attributed to their different orientation and commensurability with respect to the graphite lattice underneath (parallel or perpendicular to a main graphite axis).

In line with these observations, the distance between the tetramers along the unit cell vector a at the 1-phenylheptane–, 1-phenyloctane–, and 1-phenyldecane–solid interface is larger compared to class A solvents (4.7 nm versus 3.9 nm) (see Table 1). Actually, perpendicular to vector a , there is an excess of alkyl chains (10 instead of the expected 8 monodendron alkyl chains), which is explained by the coadsorption of two solvent molecules per tetramer colored in green and indicated with yellow arrows in Figure 3B and 3D, respectively.

Indeed, in some images (e.g., Figure 3B), small bright streaky features can be observed (indicated with yellow arrows) which we assign to the phenyl groups of the coadsorbed solvent molecules, indicated in green in the tentative molecular model in Figure 3D. These phenyl rings often appear rather fuzzy which suggests some motional freedom. Indeed, the diameter of a phenyl group (0.50 nm)¹⁶ is significantly larger than the distance between two adjacent alkyl chains (0.46 nm). Therefore, the phenyl group must be rotated out of plane. It is interesting to note that these kinds of solvent molecules alone do not show a tendency to form immobilized monolayers on graphite at room temperature. After all, this is one of the reasons why 1-phenyloctane, for example, is used as a solvent in scanning tunneling

(16) The distance between two opposing H-atoms in benzene.

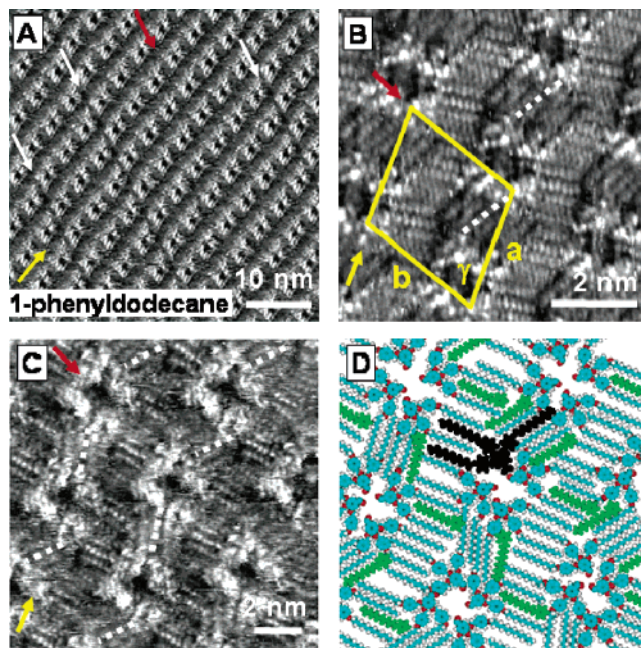


Figure 4. STM images of a monolayer of **1** physisorbed at the 1-phenyldodecane–graphite interface. (A) $I_t = 0.65$ nA; $V_t = -0.612$ V. A red arrow indicates the direction of the straight rows, and a yellow arrow indicates the wavelike rows. The white arrows indicate defect lines. (B) STM image where alkyl chains along pseudo unit cell vector a have the same orientation within the area shown. $I_t = 0.6$ nA; $V_t = -0.626$ V. The unit cell is indicated in yellow. A red arrow indicates the direction of the straight rows, and a yellow arrow indicates the wavelike rows. (C) STM image where the alkyl chains along pseudo unit cell vector a have different orientations as indicated with red lines, which leads to the wavelike pattern observed in the large scale images. $I_t = 0.55$ nA; $V_t = -0.506$ V. A red arrow indicates the direction of the straight rows, and a yellow arrow indicates the wavelike rows. (D) A tentative molecular model of the molecular organization in C. Coadsorbed solvent molecules are colored in green. Neither the exact location nor the orientation of the coadsorbed solvent molecules is known. One monodendron is indicated in black. Oligoether chains are omitted.

microscopy at the liquid–solid interface. Despite the difference in alkyl chain length of the coadsorbed solvent molecules, the monolayer patterns in 1-phenylheptane, 1-phenyloctane, and 1-phenyldecane are very similar (Table 1).

1-Phenyldodecane: In 1-phenyldodecane, the monolayers become more complex. Figure 4 represents STM images of monolayers of **1** physisorbed at the 1-phenyldodecane–graphite interface. Again, tetramers are observed. However, no 2D crystal is formed. As shown in Figure 4A, perfectly straight rows are formed along the image diagonal top left–bottom right (indicated with a red arrow in Figure 4A, i.e., along pseudo¹⁷ unit cell vector b) with a constant repeat distance ($4.7 \text{ nm} \pm 0.1 \text{ nm}$) between the tetramers. However, the rows along the image diagonal bottom left–top right show a wavelike feature (indicated with a yellow arrow, i.e., along pseudo unit cell vector a). The distance between adjacent tetramers along a wavelike row is fairly constant ($4.7 \pm 0.1 \text{ nm}$), though except at some “defects lines” indicated by white arrows in Figure 4A.

This wavelike pattern is caused by two *nonperiodic* different orientations of alkyl chains between tetramers along the wavelike diagonal (yellow arrow) in Figure 4A. The orientation of these alkyl chains is indicated explicitly by the dashed white lines in the small scale STM images in Figure 4B and 4C. The

(17) The term “pseudo” unit cell is used here because no 2D crystals are formed.

orientation of these images corresponds almost to the large scale image in Figure 4A, and equivalent directions are indicated by yellow and red arrows, respectively. The alkyl chains along pseudo unit cell vectors a and b are not perpendicular to one another, in contrast to the right angle observed between the two subsets of alkyl chains in class B solvents with shorter alkyl chains. In Figure 4B, the alkyl chains along the direction indicated by the yellow arrow have the same orientation along unit cell vector a , and as a result, the tetramers also lie perfectly on a line along that direction. However, the situation in Figure 4B is not representative for the molecular organization as observed on the scale of a domain. For instance, in Figure 4C, not all alkyl chains along the direction indicated by the yellow arrow have the same orientation and, as a result, the tetramers do not lie in a straight line along that direction. This leads to the creation of a wavelike pattern along that direction. Due to the *nonperiodic* alternation of the orientation of these alkyl chains, the wavelike patterns are *nonperiodic* too. A tentative molecular model is proposed in Figure 4D and reflects the molecular organization of part of the monolayer in Figure 4C. Note that the location of the coadsorbed solvent molecules as indicated in the model has not been determined explicitly in the STM images, as it is difficult to distinguish between the coadsorbed alkylated solvent molecules and the alkyl chains of the monodendron (see also Figure S3 in Supporting Information).

The value determined for pseudo unit cell vector a (4.7 ± 0.1 nm) is comparable to the values obtained for the shorter phenyl alkanes. Ten alkyl chains are adsorbed perpendicular to pseudo unit cell vector a instead of the expected 8 for exclusive monodendron adsorption: two molecules of 1-phenyldodecane are coadsorbed inside the 2D molecular network. The images suggest that more than two solvent molecules are coadsorbed per tetramer perpendicular to pseudo unit cell vector a (i.e. between wavelike rows), as was observed previously for the shorter solvent molecules. Often more alkyl chains are also identified along pseudo unit cell vector a (5 to 6: the exact number is often hard to quantify due to image contrast issues, e.g. Figure 4C), indicating that 1 or 2 solvent molecules are coadsorbed between the tetramers along this pseudo unit cell vector, therefore along the wavelike row. The peculiar orientation of the alkyl chains along unit cell vector a might be caused by a mismatch between the length of the coadsorbed 1-phenyldodecane solvent molecules perpendicular to unit cell vector a and the length of the monodendron's alkyl chains.

1-Phenyltetradecane: Figure 5 represents high-resolution STM images of a physisorbed monolayer of **1** at the 1-phenyltetradecane–graphite interface. Also in this case, cyclic tetramers are formed (individual phenyl groups can easily be distinguished), though it is clear that the monolayer structure differs again significantly from those observed in the other solvents. The number of alkyl chains along unit cell vector a has increased to typically 8, compared to 4 in the case of 1-phenylheptane, 1-phenyloctane, and 1-phenyldecane (lower half of Figure 5A/upper half of Figure 5B), though sometimes only 5 alkyl chains bridge the gap between two tetramers along unit cell vector a (upper part of Figure 5A/lower part of Figure 5B). A few sets of alkyl chains are indicated in red in Figure 5A. When 8 alkyl chains bridge the gap between two tetramers, at least 6 solvent molecules per tetramer are coadsorbed: 2 at

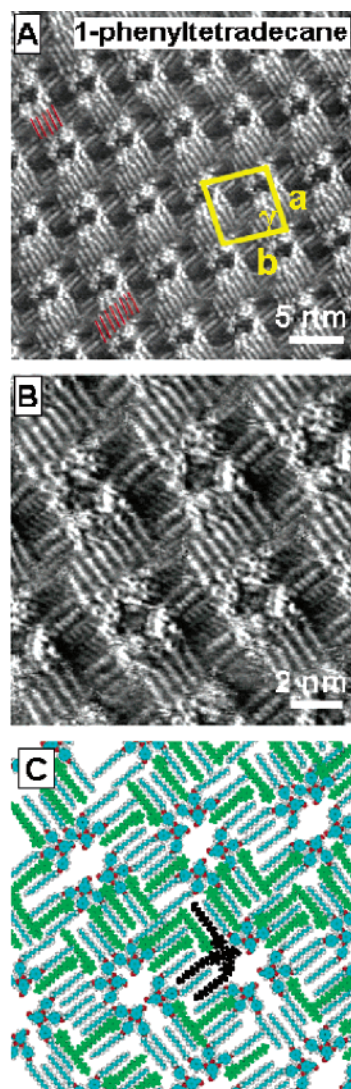


Figure 5. STM images of a monolayer of **1** physisorbed at the 1-phenyltetradecane–graphite interface. (A) $I_t = 0.65$ nA; $V_t = -0.290$ V. A few sets of alkyl chains are indicated in red. A unit cell is indicated in yellow reflecting the situation where eight alkyl chains are observed along unit cell vector a . (B) $I_{set} = 0.65$ nA; $V_{set} = -0.428$ V. (C) A tentative molecular model. The codeposited solvent molecules are indicated in green. Neither the location nor the orientation of the coadsorbed solvent molecules is known. One monodendron is indicated in black. Oligoether chains are omitted.

both sides of the tetramer along unit cell vector a and 2 at each side of the tetramer perpendicular to unit cell vector a . On the other hand, when 5 alkyl chains bridge the gap between two tetramers, 4 solvent molecules per tetramer are coadsorbed: 1 along unit cell vector a and 3 perpendicular to unit cell vector a . These differences are reflected in the unit cell area (Table 1). A tentative molecular model is proposed in Figure 5C where solvent molecules are indicated in green. Note that, in this complex organization, neither the exact location nor the orientation of the coadsorbed solvent molecules is completely identified.

Dodecane and Tetradecane: Experiments have also been performed in two hydrophobic solvating hydrocarbons such as dodecane and tetradecane, respectively, to investigate the 2D molecular ordering of **1** and to probe the importance of the phenyl group of the solvent molecules.

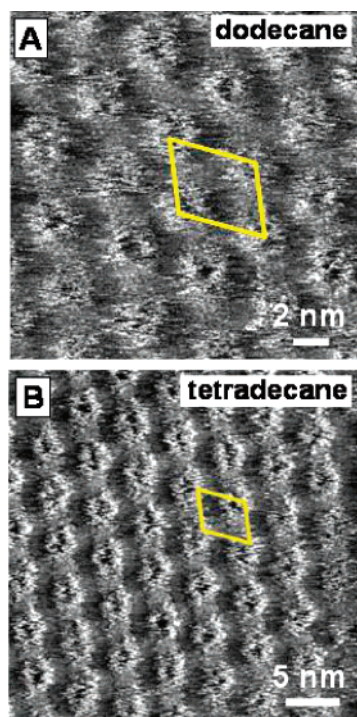


Figure 6. (A) STM image of a monolayer of **1** physisorbed at the dodecane–graphite interface. $I_t = 0.6$ nA; $V_t = -0.420$ V. (B) STM image of a monolayer of **1** physisorbed at the tetradecane–graphite interface. $I_t = 0.65$ nA; $V_t = -0.728$ V.

Figure 6A and 6B illustrate STM images recorded for adlayers of **1** physisorbed at the dodecane–graphite interface and tetradecane–graphite interface, respectively. Although the resolution of the STM images in these two solvents is far from ideal, individual tetramers can still be identified. No unit cell parameters are given as no internal calibration with the graphite substrate could be obtained. However, the symmetry and approximate size of both unit cells are comparable to those obtained in 1-phenyloctane. For instance, from row to row, no apparent change in the orientation of the tetramers was observed. These observations strongly suggest that solvent molecules might be coadsorbed although they are not identified in the STM images.

4. Discussion

Table 1 summarizes the characteristic parameters of the 2D self-assembled patterns of physisorbed adlayers of monodendron **1** in the different solvents used in this study.

4.1. Why Tetramers? The formation of cyclic tetramers of monodendron **1** is clearly observed in many alkylated solvents with hydrophilic solvating as well as with hydrophobic solvating functional groups. At the liquid–solid interface, the supramolecular structures are the result of a delicate balance between the molecular shape and composition and molecule–molecule, molecule–substrate, and solvent interactions. The monodendrons are amphiphilic in nature, with a rather hydrophilic oligoether apex and hydrophobic phenyl–alkyl moieties in the periphery. The solvents used are not ideal to solubilize the hydrophilic oligoether. Clearly, the formation of tetramers where the oligoether moieties are “clustered” in the center of the cavity is one of the efficient ways to optimize their interaction. In addition, intermolecular hydrogen bonding interactions between a hydroxyl group and a carbonyl group of the apices are

possible. The presence of many alkyl chains further leads to stabilizing interactions with the graphite substrate, which clearly has an effect on their ordering: the alkyl chains perpendicular to unit cell vector a run parallel with one of the major symmetry axes of graphite; those along unit cell vector a are oriented perpendicular to the major graphite axis (except for monolayers of **1** in 1-phenyldodecane). To maximize the substrate coverage, which is favored for enthalpic reasons, alkyl chains of different monodendrons in adjacent tetramers are interdigitated, giving rise to a closely packed structure and favorable van der Waals interactions between the alkyl chains.

4.2. The Orientation and Shape of the Tetramers and the Effect of Solvent Codeposition. The structure and orientation of the tetramers are clearly solvent dependent. If no solvent molecules are coadsorbed, the orientation of the tetramers alternates from row to row. This alternation in 1-octanol, for instance, seems to be the result of packing constraints: optimal van der Waals contacts can be realized between the interdigitating alkyl chains leading to a perfect fit if the orientation of the tetramers is alternated from row to row. However, upon solvent codeposition, more squarelike tetramers are formed, and no such alternation is observed. Coadsorption of solvent molecules perpendicular to unit cell vector a leads to an increase in the distance between adjacent tetramers along that unit cell vector. Therefore, coadsorption of the alkylated solvent molecules allows also the alkyl chains of monodendron **1** along the unit cell vector a direction to be fully adsorbed on graphite, which maximizes the interaction of the adsorbate with the graphite lattice. Note that, in all cases, the monolayers are chiral (unit cell is oblique). The supramolecular tetramers are most likely chiral too. In the case no solvent molecules are coadsorbed, this is obvious from the clear row to row alternation (e.g., Figure 2B).

4.3. Monolayer Formation: The Nature of the Solvent.

As discussed above, solvent coadsorption of the phenyl-substituted alkanes and likely also for the n -alkanes (class B) favors close-packed monolayer formation and allows all alkyl chains of the monodendrons to be fully adsorbed on the graphite surface. Despite the fact that, for alkane derivatives with hydrophilic solvating functional groups (class A), no solvent coadsorption takes place, monolayer formation is observed, which according to our hypothesis can be understood in terms of (1) the interaction of the hydrophilic solvating functional groups of these solvent molecules (OH and COOH) with the hydrophilic interior of the tetramers and (2) intermolecular hydrogen bonding. In 1,2,4-trichlorobenzene (data not shown), such solvent-induced stabilization is not possible, and no monolayers are formed.

The question arises as to why, in class A solvents, no solvent molecules are coadsorbed, while in class B solvents, solvent coadsorption is observed, despite the fact that in all cases the solvent molecules are alkylated. Clearly, the nature of the functional group must play a key role. A favored interaction of unsubstituted and phenyl-substituted alkyl chains with the substrate is unlikely compared to OH or COOH functionalized alkyl chains. On the contrary, it is possible to observe, for example, the monolayer formation of 1-octanol molecules in pure solvent conditions. This is never observed for 1-phenyloctane molecules under comparable experimental conditions. In addition, sometimes 1-octanol molecules are coadsorbed, for

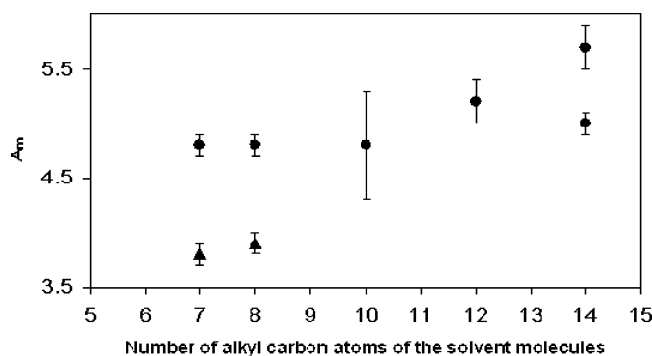


Figure 7. The graph represents the evolution of A_m (the unit cell area divided by the number of monodendrons per unit cell), as a function of the nature of the solvent and the length of the alkyl chains. Triangular and circular dots indicate solvents of class A and B, respectively.

instance, in the presence of 5-alkoxy-isophthalic acids.^{4a} In those cases where 1-octanol molecules could be observed on a surface, they are stabilized by intermolecular hydrogen bonding *in the sample plane*: in 1-octanol monolayers, hydrogen bonds are formed between the OH groups while, in mixed monolayers with 5-alkoxy-isophthalic acid, the interactions between the OH group of the alcohol and the COOH group of the 5-alkoxy-isophthalic acid stabilize the mixed patterns. In the case of monodendron **1**, coadsorption of the hydrophilic solvating alkylated solvents (class A) could actually be disfavored: stabilization of the OH or COOH groups by intermolecular hydrogen bonding between physisorbed molecules on the substrate is not possible. On the contrary, the OH or COOH groups of hypothetically coadsorbed hydrophilic solvent molecules would interact by intermolecular hydrogen bonding with other solvent molecules or monodendrons in the solution, hence destabilizing their coadsorption. Further support for the important role played by the OH group is gained from experiments in 6-phenyl-1-hexanol, where monolayer formation is observed, though without coadsorption of the solvent molecules (see also Figure S4 in the Supporting Information).

4.4. The Effect of Alkyl Chain Length. In the class A solvents investigated, no chain length dependence on the monolayer formation was observed. This is not surprising as these solvents have similar properties. Moreover, **1** forms a densely packed monolayer in these solvents without any space for solvent codeposition. This system is clearly different from the system reported by Lackinger et al.⁶ where trimesic acid shows polymorphism depending on the length of the alkyl chains of the solvent molecules. An important difference, however, is that trimesic acid forms an open network. In that case, solvent molecules can interact with the substrate in the void areas.

Figure 7 displays A_m , the unit cell area divided by the number of monodendrons per unit cell, as a function of the alkyl chain length of the solvent molecules. The value of A_m for class A solvents is smaller than that for class B solvents, reflecting the coadsorption of solvent molecules in the case of class B solvents.

However, the molecular packing density is very similar in both cases: for instance, the difference in A_m between 1-heptanol and 1-phenylheptane (1 nm²) matches very well with the calculated area occupied by the sum of half of a solvent molecule and a dodecyloxy chain (see Supporting Information S5).

The number of coadsorbed solvent molecules and the supramolecular pattern formed depend on the alkyl chain length,

which is also reflected by the value of A_m (see Table 1 and Figure 7): in the case of class B solvents, A_m increases with increasing alkyl chain length of the solvent molecules. However, within experimental error, the value of A_m for 1-phenylheptane, 1-phenyloctane, and 1-phenyldecane is identical. Therefore, the packing density for 1-phenyldecane will be slightly higher than that for 1-phenylheptane.

The question arises as to why the packing motifs are identical for the shorter phenylalkanes ($n \leq 10$) but differ for 1-phenyl-dodecane and 1-phenyltetradecane. Apparently, if the length of the coadsorbed solvent molecules exceeds the length of the monodendron alkyl chains significantly, there is not enough space for the solvent molecules to coadsorb in the same way as the shorter 1-phenylalkanes. Compare the length of 1-phenyl-octane (1.48 nm), 1-phenyldecane (1.73 nm), 1-phenyldodecane (1.97 nm), and a dodecyloxy chain of monodendron **1** (1.56 nm) (Supporting Information S5). Due to the greater than 30% difference in length between a dodecyloxy chain and 1-phenyl-dodecane chain, it's not surprising that a different behavior is observed in this solvent compared to the class B solvents with shorter alkyl chains.

Initially, it was anticipated that increasing the length of the alkyl chains of the solvents would eventually disfavor the formation of a monolayer or at least solvent coadsorption due to a mismatch of the length of the solvent molecules and the dodecyloxy chains of the monodendron. Surprisingly, in the case of 1-phenyldodecane and 1-phenyltetradecane, solvent molecules are still coadsorbed and even more than for the shorter 1-phenylalkanes, which is reflected by an increased value of A_m . Note that the adsorption energy of alkanelike molecules on graphite increases almost linearly with chain length due to the close registry between the carbon backbone and the graphite lattice.¹⁸ Thus, increasing the length of the alkyl chains favors coadsorption of the solvent molecules as their interaction with the substrate increases. However, unfavorable steric interactions, which might arise due to a difference in length between the solvent molecules and the alkyl chains of the monodendrons, are relieved by changes in the 2D packing. For example, in the case of 1-phenyldodecane the coadsorbed solvent molecules and dodecyloxy groups along pseudo unit cell vector *a* do not run parallel with this unit cell vector.

Conclusions

The 2D supramolecular self-assembly of monodendron **1** is solvent dependent, both with respect to the nature of the solvent (hydrophilic solvating versus hydrophobic solvating; hydrogen-bond forming or not) and with respect to the length of the alkyl chains of the solvent molecules in the case of coadsorption.

Upon adsorption of monodendron **1** at the liquid–graphite interface, cyclic tetramers are formed. The formation of tetramers has been rationalized in terms of the monodendron shape and specific noncovalent stabilizing interactions of the hydrophilic (oligoether - hydroxyl) and hydrophobic (alkyl - aromatic) groups of the solute with the solvent and substrate.

In aromatic alkylated solvents and *n*-alkanes, solvent molecules are coadsorbed and are part of a complex 2D molecular network. However, in alkylated alcohols and acids, no solvent

(18) (a) Paserba, K. R.; Gellman, A. J. *J. Chem. Phys.* **2001**, *115*, 6737. (b) Paserba, K. R.; Gellman, A. J. *Phys. Rev. Lett.* **2001**, *86*, 4338. (c) Müller, T.; Flynn, G. W.; Mathauser, A. T.; Tepljakov, A. V. *Langmuir* **2003**, *19*, 2812.

codeposition is observed. The difference in coadsorption behavior of hydrophilic solvating and hydrophobic solvating alkylated solvents has been explained in terms of specific interactions between solvent molecules: without in plane stabilizing interactions, hydrogen-bond forming solvents do not coadsorb.

The number of coadsorbed solvent molecules depends on the length of the aliphatic chain of the solvent and was generally found to increase upon increasing the alkyl chain length of the phenyl alkanes, reflecting a balance between solvent–substrate interactions and steric constraints.

In summary, we have demonstrated the importance of the choice of solvent on the monolayer formation of amphiphilic molecules at the liquid–solid interface and provided insight in the role played by (1) the solubilizing nature of the solvent (solvent–solute interactions), (2) specific solvent–solvent interactions, and (3) the solvent dimension (length of the alkyl chain).

A priori, it's hard to predict the influence of the solvent on the pattern formation. For some systems, the choice of the solvent will not make any difference in the pattern formation, while, for other systems, it will be crucial. Thermodynamics and kinetics play a role, and several polymorphous structures can be formed. Despite the difficulties in predicting the effect of the nature of the solvent on the monolayer formation for a particular system, some general remarks can be made: (1) The monolayer formation process and the monolayer structure are more difficult to predict as the structural and functional complexity of the molecules increases. This is true with respect to both the solute and the solvent. (2) The stronger the

adsorbate–adsorbate interactions compared to the solute–solvent interactions, the weaker the role of the solvent on the monolayer formation. (3) Solvent molecules with some structural (e.g., alkyl chains) or functional properties (hydrogen bonding groups,...) which complement or interact with those of the solute might have an important effect, e.g., by coadsorption. (4) Adsorbates forming an open network are more prone to solvent effects than those forming a closely packed network. (5) Important solvent effects can be anticipated if the adsorbate is amphiphilic in nature.

In general, an understanding of solvent effects will allow us to direct and control the molecular ordering of 2D physisorbed monolayers, a topic of major importance. For the current system, this might be exploited for the formation of 2D templates where the tetramers act as hydrophilic containers.

Acknowledgment. The authors thank the Federal Science Policy, through IUAP-V-03, and the Fund for Scientific Research-Flanders (FWO). V.P. and A.D. thank the National Science Foundation (USA) for financial support. W.M. and H.U. are grateful to KULeuven (Interdisciplinary Research Program) for financial support. S.D.F. is a Postdoctoral Fellow of FWO.

Supporting Information Available: Extra STM images of different sizes and of monolayers of **1** at the 6-phenyl-1-hexanol/graphite interface, and calculations on surface area (PDF). This material is available free of charge via the Internet at <http://pubs.acs.org>.

JA056175W